

**AN EVAPORATION DEPOSITION  
SYSTEM FOR THE IN-SITU STUDY  
OF THIN METAL FILMS**

By

Joshua David Mertzluft

A thesis submitted in partial fulfillment of the  
requirements for the degree of

Bachelor of Science

Houghton College

August 2013

Signature of Author.....

Department of Physics  
August 23, 2013

.....

Dr. D. Brandon Hoffman  
Assistant Professor of Physics  
Research Supervisor

.....

Dr. Mark Yuly  
Professor of Physics and Department Chair

**AN EVAPORATION DEPOSITION  
SYSTEM FOR THE IN-SITU STUDY  
OF THIN METAL FILMS**

By

Joshua David Mertzlufft

Submitted to the Department of Physics  
on August 23, 2013 in partial fulfillment of the  
requirement for the degree of  
Bachelor of Science

**Abstract**

Thin films have been the subject of study for years by research groups both in academia and the semiconductor industry. With applications primarily in microelectronics and also emerging applications in the energy industry, it is desirable to have a greater understanding of the underlying characteristics of the films. This project is focused on the construction of a deposition system that may be used to produce thin films for study at Houghton College, a small Christian liberal arts institution. The system will also enable researchers to study the effects of annealing in-situ.

Thesis Supervisor: Dr. D. Brandon Hoffman  
Title: Assistant Professor of Physics

## TABLE OF CONTENTS

<b>Table of Contents .....</b>	<b>3</b>
<b>Table of Figures .....</b>	<b>5</b>
<b><i>Chapter 1. Introduction.....</i></b>	<b>6</b>
<b>1.1 Description of Thin Metal Films .....</b>	<b>6</b>
<b>1.2 History and Background of Research .....</b>	<b>6</b>
<b><i>Chapter 2. Thin Films .....</i></b>	<b>12</b>
<b>2.1 Crystal Lattice Structures in Thin Films .....</b>	<b>12</b>
<b>2.2 Stresses in Thin Films .....</b>	<b>15</b>
<b><i>Chapter 3. Apparatus.....</i></b>	<b>18</b>
<b>3.1 Overview .....</b>	<b>18</b>
<b>3.2 Vacuum Technology .....</b>	<b>18</b>
3.2.1 Rotary Vane Pump.....	19
3.2.2 Turbomolecular Pump .....	21
3.2.3 Ion Pump.....	24
3.2.4 Vacuum Gauges .....	25
<b>3.3 Internal Components.....</b>	<b>26</b>
3.3.1 Evaporation Block .....	26
3.3.2 Sample Substrate Heater/Holder.....	28
3.3.3 Evaporation Rate Monitor .....	31
3.3.4 Ion Mill.....	34
3.3.5 Rotary and Linear Shutters .....	35
<b>3.4 Suspension of System .....</b>	<b>35</b>
<b>3.5 The Interferometer .....</b>	<b>35</b>
<b><i>Chapter 4. Current Status of the Project.....</i></b>	<b>39</b>

4.1	Overview .....	39
4.2	Components Remaining to be Completed .....	39
	<i>Chapter 5. Conclusions</i> .....	40
	Appendix I .....	41
	AI. 1 Pump-Down Procedure .....	41
	AI.2 Venting Procedure .....	42
	References .....	43

## TABLE OF FIGURES

Figure 1: Thin Film Definition .....	6
Figure 2: A.W. Wright's 1877 Sputtering apparatus.....	9
Figure 3: Edison's device for providing a base coating of metal for phonograph records.....	10
Figure 4: Electron microscope view of a tri-gate transistor .....	11
Figure 5: Diagram of a face-centered cubic (FCC) crystal.....	12
Figure 6: Diagram depicting the two general orientations of silver crystals .....	13
Figure 7: Isometric diagram 100 orientation silver crystals arranged in a square lattice .....	14
Figure 8: Current theory claims there is a critical thickness ( $t$ ) in thin films.....	16
Figure 9: Observed data shows that there is always a combination of 111 and 100 crystals.....	17
Figure 10: The Houghton College PVD chamber.....	19
Figure 11: The Rotary Vane Pump.....	20
Figure 12: Cross-section diagram of the turbomolecular pump .....	23
Figure 13: A cutaway of a common turbomolecular pump.....	23
Figure 14: Ion Pump. Molecules enter the apparatus and ionized .....	24
Figure 15: The deposition block system.....	27
Figure 16: Initial method of filament threading through the sample heater disc .....	29
Figure 17: Alternate method of filament threading through the sample heater disc .....	29
Figure 18: The Sample Substrate Holder/Heater Assembly .....	30
Figure 19: Evaporation Rate Monitor.....	33
Figure 20: The Twyman-Green interferometer basic optics setup.....	37
Figure 21: The mounted chamber and interferometer.....	38

## Chapter 1.

### INTRODUCTION

#### 1.1 Description of Thin Metal Films

Thin films are defined as materials configured in such a way that the planar dimensions vastly exceed the dimension normal to the plane. In other words, the thickness ( $z$ ) is much smaller than the width ( $x$ ) or length ( $y$ ). The film thickness is also considered negligible compared to the surface of the substrate, as shown in Figure 1. These thin films exhibit many interesting properties that normal materials do not easily exhibit. One of these is their ability to be structurally transformed by annealing at relatively low temperatures (lower than 500K). These structural changes can theoretically be leveraged to improve structural integrity or electrical conductivity. The applications of such improvements to the thin film follow very quickly in the modern area of microelectronics and the growing area of nanoelectronics.

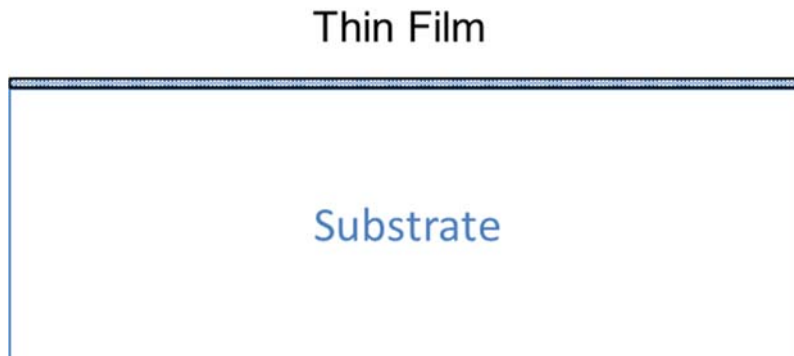


Figure 1: For a film to be considered thin, the planar dimensions far exceed the normal dimension. Its thickness may also be considered insignificant compared to the substrate to which it is deposited on.

#### 1.2 History and Background of Research

Thin films have been a subject of scientific curiosity for many generations [1]. With the many applications of creating sustainable and ideal thin films ranging from improving electrical

conductivity of metals used in electronics [2] to creating smaller electronic systems to developing energy storage units with greater capacity [3], it is clear that there is a benefit to learning how to manipulate the characteristics of the films.

With advances in modern science, researchers have been able to conduct very extensive research on these films in highly controlled environments. Often, metal films are made in either high vacuum or ultra-high vacuum (UHV) chambers using a physical vapor deposition process. [1][4]

The physical vapor deposition (PVD) process works on the simple principle of evaporation and adsorption. In a typical PVD system, the deposition material is placed in standard temperature and pressure (STP) form in a crucible near the bottom of a closed chamber. Inside that chamber, near the top and facing down, is a silicon substrate. The chamber is evacuated and the deposition material is heated to the temperature at which it begins to evaporate. Some of that vapor adsorbs to the substrate and at a controlled thickness, this condensed vapor is what makes up the thin film.

There has been over a century of development leading up to what we consider a modern PVD system, most notably in the field of vacuum technology. Interestingly enough, the concept of thin film deposition is believed to be discovered by accident in the mid-eighteenth century. In 1852, W. Grove noted a strange phenomenon that occurred during his experiments with electrodes [5]. After this phenomenon was observed, scientists such as Faraday, Plücker, and Wright began to experiment with it purposefully. Faraday concerned his experiments with the optics of these films, observing the transmission, refraction, and reflection effects of films of various metals on polarized light waves [6]. Plücker noted a “beautiful metallic mirror” formed of platinum on the inside of a discharge tube [7]. Wright was one of the first to purposefully investigate the concept of electrical deposition itself, creating one of the first apparatuses for the sole purpose of sputtering (depicted in Figure 2). Wright’s apparatus consisted simply of a vacuum chamber as well as a substrate and electrodes. Once evacuated (to control the environment as well as remove impedance from normal atmospheric conditions), Wright used the electrodes to emit, or sputter, atoms of the cathode’s mass, directed towards the anode in the lower portion of the chamber, with the intent of collecting a portion of these atoms on a substrate. In addition to this, his chamber was able to be rotated to

move the substrate out of the way of the primary flow of mass from the cathode to the anode for purposes of collecting differing amounts of mass on the substrate itself [9].

Further along in the development of thin film technology, scientists and engineers, such as Thomas Edison began to apply the developing technology in commonly known products. Edison sought a method of creating stronger phonograph records and to do so he decided the best solution was to coat them with a thin layer of metal. He understood that the common process of electroplating could be used to coat the records with a protective layer of metal. However the records by themselves were not electrically conductive enough for the more practical and heavy-duty method of electroplating to take place. He knew of the rising field of vapor deposition and patented a method that utilized this concept in vacuum to provide a base metallic coating for his phonograph records (depicted in Figure 3).

Edison's device was somewhat crude by today's standards as its only purpose was to provide a coating on an apparatus, but nonetheless it provides a foundation for many modern uses of thin metal films in the industry. Edison's device functioned using a glass bell jar vacuum chamber. The vacuum chamber was used to maintain as much purity as possible, as well as shield the delicate process from external ambient conditions, therefore allowing Edison to tightly control the conditions in which his deposition would take place. Contained inside this chamber was the apparatus to be coated as well as electrodes which have a current run through them such that they emitted atoms from their own mass which were electrically attracted to the grounded target apparatus [8]. Thus Edison was able to successfully coat non-conductive records with a protective electroplated metal coating using this thin conductive base layer.



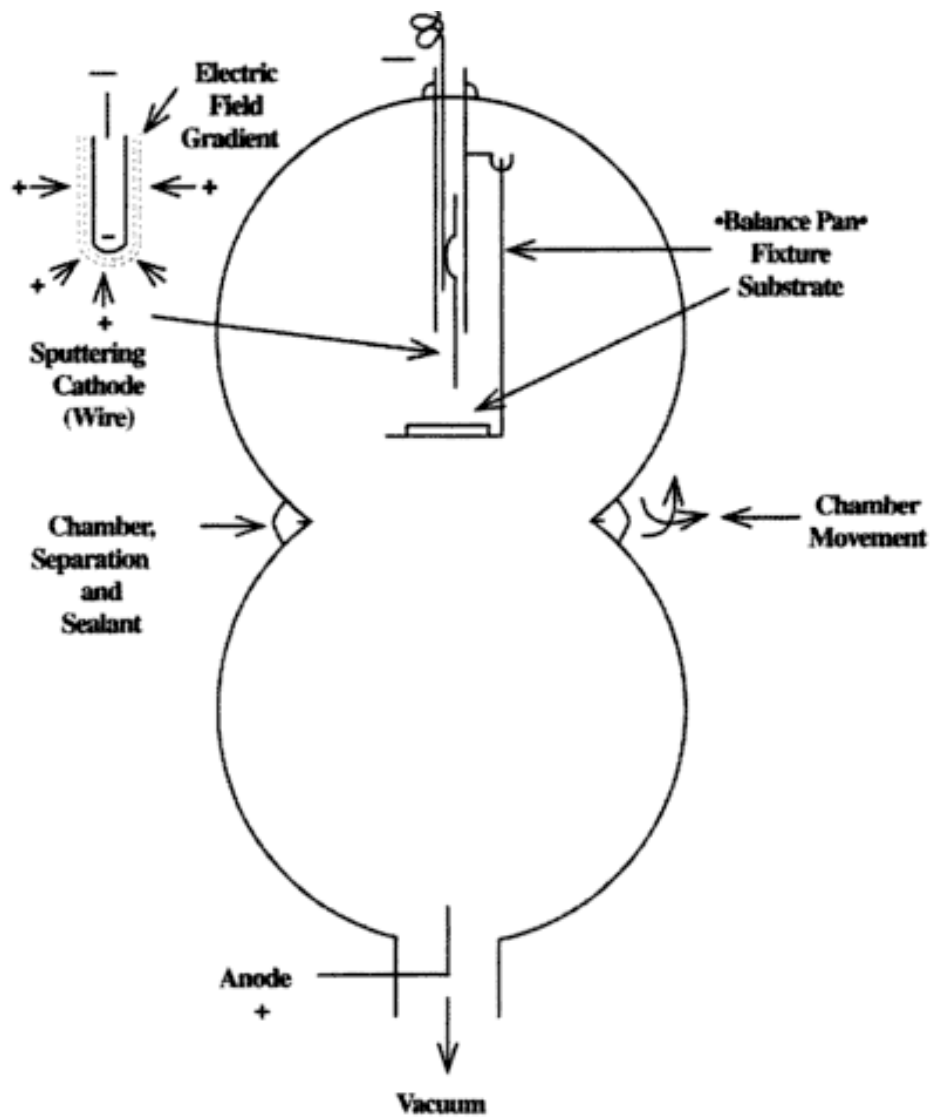


Figure 2: A.W. Wright's 1877 Sputtering apparatus. This denotes the early development of film deposition in vacuum. Atoms travelled from the electrical cathode to the anode, and the substrate could be moved in and out of this flow. Figure taken from Ref. [9].

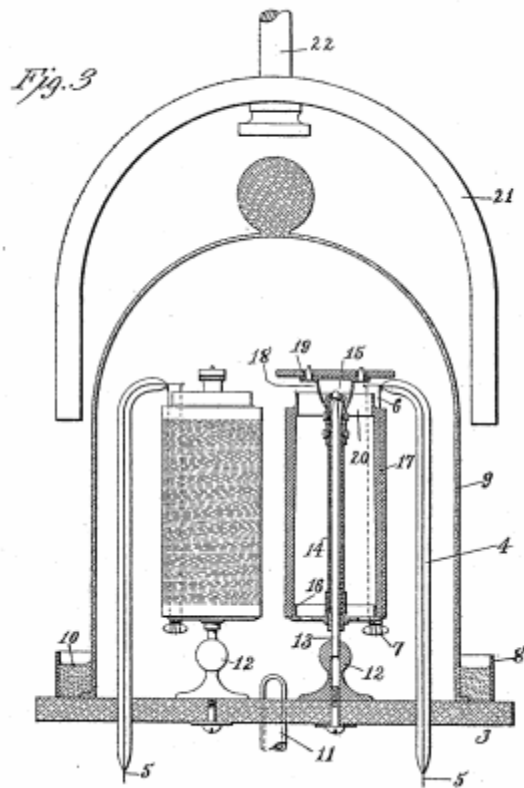


Figure 3: Edison's device for providing a base coating of metal for phonograph records using the concept of PVD. The vacuum chamber was used to maintain as much purity as possible, as well as shield the delicate process from external ambient conditions, therefore allowing Edison to tightly control the conditions in which his deposition would take place. Contained inside this chamber was the apparatus to be coated as well as electrodes which have a current run through them such that they emitted atoms from their own mass which were electrically attracted to the grounded target apparatus. Figure taken from Ref. [8].

Moving forward into modern times, physical vapor deposition has become a common process in industry. Today's technology industry owes most of its success to the advancements in thin film technology enabling circuits to be made smaller and less expensive. A clear example of this advancement is in microprocessors. The first common-use 8086 developed by Intel in the 1970's had a smallest component measuring a few micrometers, nearly a hundred times larger than the company's current Ivy bridge architecture, which boasts components measuring a mere 22nm! [10]

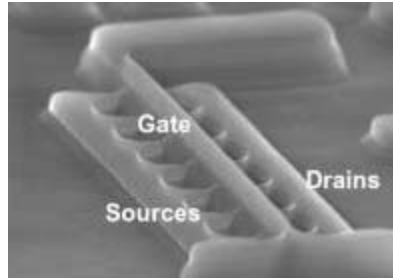


Figure 4: Electron microscope view of a tri-gate transistor. Developed by Intel on the 22nm architecture scale. Figure taken from Ref. [10].

With component size shrinking further and further, there is a greater and greater need to understand the characteristics of materials on this nano scale. Professors at many large universities have taken up this challenge, including the Massachusetts Institute of Technology [12] and Cornell University [13] (some of which is discussed in chapter two of this manuscript), all discovering new characteristics that show materials are not the same on the scale of nanometers as they are in the common scale.

This need is also the reason that the Hoffman Research Group at Houghton College, a small Christian liberal arts school, is currently in the process of assembling a laboratory which may be used to study and develop thin film technology. Once films are produced, there are a series of methods used for studying them ranging from x-ray diffraction to atomic force microscopy to laser interferometry; all of which will be also constructed at Houghton College. Gaining and understanding of the underlying crystal structures of the films and the force per unit area (stresses) due to temperature variance, both of which are discussed later in chapter two, will allow the group to add to the community's understanding of films. In order to study the films, it is desirable for the group to have a viable and consistent system to procure films.

*Chapter 2.*

THIN FILMS

**2.1 Crystal Lattice Structures in Thin Films**

As the Hoffman group is primarily interested in studying the effects of annealing metal films, an essential knowledge of the properties of thin film texture is required. As the first metal to be studied is silver, it will be used as a physical example throughout this section. At such a thin layer, it becomes necessary to observe films as iterations of their characteristic crystal structure. A crystal structure is defined as an array of atoms forming a solid. It is important to note that the base element of the crystal structure is periodic in that it repeats in all Cartesian dimensions to form the total crystal structure. There are multiple known crystal structures, as different atoms take on several different configurations when assembled together. For example, atoms of silver form in iterations of face-centered cubic (FCC) crystals (see Figure 5). In an FCC crystal, one can imagine a cube with an atom at each corner with one at the center of each square face.

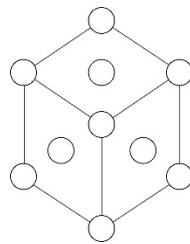


Figure 5: Diagram of a face-centered cubic (FCC) crystal. Such a crystalline structure can be observed in silver

When studying silver crystals, they are generally described by their Miller indices. A crystal's Miller index describes its orientation relative to the desired coordinate axes. Observation of a single face and how it intersects the axes is determinative of the orientation geometry. In Figure 6, the planes defined by these crystal faces, parallel to the surface of the substrate, are shown in two

different orientations which are described by Miller indices. The Miller index of a given crystal structure is defined in the following way:

$$hkl = \left( \frac{1}{x_1}, \frac{1}{x_2}, \frac{1}{x_3} \right), \quad (1)$$

where  $h$ ,  $k$ , and  $l$  are the Miller indices of the crystal face and  $x_1$ ,  $x_2$ , and  $x_3$  are the normalized coordinates of the crystal lattice at which the face intersects the x, y, and z axes, respectively. A special case exists where the face never intersects a given axis. Frequently, the case occurs where a face runs parallel to a respective axis and therefore never crosses it. Such a plane's characteristic value  $x_n$  for any plane running parallel to an axis  $n$  is said to be infinity. [11]

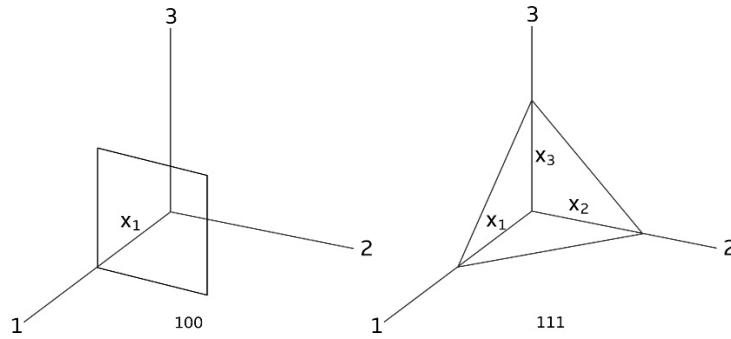


Figure 6: Diagram depicting the two general orientations of silver crystals. The 100 plane only intersects one crystal axis while the 111 plane intersects all three.

In general two orientations are considered for the purposes of studying of thin silver films. The 100 orientation is used to describe crystal structure faces that only intersect a single axis. The second orientation considered, 111, is if the crystal plane intersects equidistant from the origin on all three axes. In Figure 6, the two orientations are shown. The planes shown are always considered to be parallel to the substrate. On the left, the 100 orientation shows that its plane intersects only one

axis. The diagram on the right exhibits the 111 orientation; the plane of which intersects all three axes due to its skew.

The crystal lattices formed by these orientations can be viewed as groupings of six-sided dice that are held together. In the 111 orientation, the dice are standing on their corners and in the 100 orientation they are lying flat on their faces. This square grid of 100 orientation crystals (as seen in Figure 7) is believed to have greater strength and electrical conductivity than the 111 orientation.

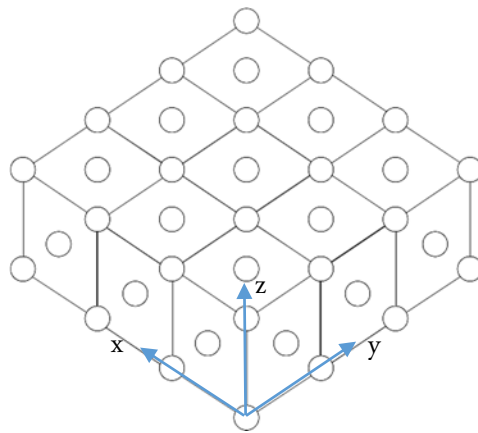


Figure 7: Isometric diagram 100 orientation silver crystals arranged in a square lattice. It is 100 because the crystal surfaces align with the origin (x,y,z) datum planes.

When a silver film is produced, most of the crystals are characterized by the 111 orientation. It has been shown that this silver crystal structure can be manipulated by the process of annealing. At first, the group will be specifically studying the effects of heating on the transition of a silver film from being mostly 111 to mostly 100. Typically, this annealing is performed post-deposition and in different environment, which subjects the film to atmosphere. The system described herein is different in that will allow the group to study the films without moving them from their deposition location and environment.

## 2.2 Stresses in Thin Films

Since thin silver films' crystal structures can be observed in several different orientations, it is desirable to be able to control the orientation of the silver in the film. When deposited, the crystal lattice of the film is usually determined to be almost completely in the 111 Miller Index orientation. The effect of the transformation process is to change the orientation from mostly 111 to mostly 100.

A current model of thin silver films, described by C.V. Thompson in [12] makes the statement that the film must be fully 111 or fully 100, but can't be anything in between and will only transform if the film thickness is greater than a certain value. This theory is visualized in Figure 8. A film must be either fully 111 or fully 100. This theory is based on the concept of energy minimization- the film is entropic in that the favorable crystal structure is the orientation that minimizes stresses in the film. In other words, either 111 or 100 will cause the net energy in the film to be minimized. Two of the major energies contributing to the net energy in the film are the interface energy and the strain energy. Interface energy is associated with the boundary between the crystal structure of the film and the substrate and is related to the asymmetry produced by the loss of effectiveness of the lattice.

The strain energy is similar to mechanical energy stored in a spring in that it results when stresses cause the crystal lattice to experience strain, or deformation from its equilibrium state. As the system changes temperature, the differing expansion rates of the film and substrate cause the film to be stretched or compressed in the dimensions parallel to the substrate. This is the strain, being that strain is defined as the ratio of the changes in lengths of two different grains (film-film or substrate-film boundaries). This the strain in the film ( $\epsilon_x$ , in the x-direction for example) is mathematically dependent on the deformation in the stress free lattice dimension (distance between lattice iterations with no stress). That is to say that it a relationship of the film under stress ( $a_s$ ) and film in equilibrium ( $a_i$ ), given in Equation 2 for the  $x$  dimension. [4]

$$\epsilon_x = \frac{a_{s,x} - a_{f,x}}{a_{f,x}} \quad (2)$$

Stress is the restoring pressure in the film causing it to tend towards returning to its own equilibrium state, and is the result of strain, and like pressure, is equal to the force per unit area (shown in Equation 3). Typically when referring to stress in thin films, it is on the order of megapascals (MPa) or gigapascals (GPa).

$$\sigma = \frac{F}{A} \quad (3)$$

Note that stress and strain do occur in the substrate as well, but the primary focus is on the film. In fact, the example of the spring described above is considered to be accurate enough that the same Hooke's Law is used to relate stress and strain:

$$\sigma_x = M\epsilon_x, \quad (4)$$

Where  $\sigma$  is the stress induced in the film by the strain  $\epsilon_x$ . They are directly related by the biaxial modulus,  $M$ , similar to a spring constant. This constant  $M$  varies based on both the material in question as well as the crystal structure. This stress is directly related to the total interface energy in the current thin film model in that since the film-substrate system tends towards a minimal combination of interface energy and stress. [1]

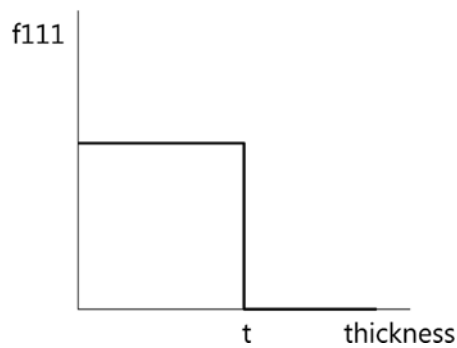


Figure 8: Current theory claims there is a critical thickness ( $t$ ) beyond which a film will transform and before which it will not. The area fraction of the 111 ( $f_{111}$ ) orientation is shown on the vertical axis and thickness is on the horizontal axis.



Particular to the current model, the strain energy depends on the thickness of the film and is what is responsible for the concept of the critical thickness.

However, this theory does not represent the observed phenomenon. Though the theory assumes ample time and energy are provided so that the film can reach its final equilibrium state, observations by the Baker Research Group at Cornell University [13] do not show a cutoff thickness that a film must be at least at or greater to transform, even with liberal amounts of time and energy. Rather the data shows that when transforming, there will always be a fraction of both 111 and 100 orientation crystals [14]. This means that the transformation function should not have a cutoff, but it should look like a smooth curve, as seen in Figure 9.

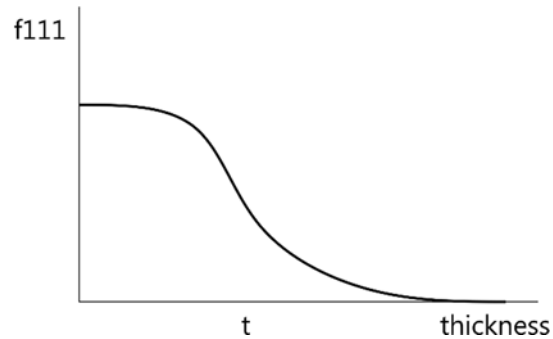


Figure 9: Observed data shows that there is always a combination of 111 and 100 crystals that make up the film, but the ratio of the two orientations changes as thickness is changed.

The deposition/interferometer system under construction at Houghton College will allow researchers to study this theory and others. The primary concept which will be employed is the heating of the film to observe both the stresses induced in the film as well as the effects of those stresses on the film's crystal structure.

*Chapter 3.*  
APPARATUS

### 3.1 Overview

In 2007, the Hoffman Research Group began work on components of a PVD system that has by the current time been assembled and is currently undergoing tests of the deposition system. The system is centered around the basic vapor deposition process: vaporizing a material and condensing that vapor on a substrate, all within a vacuum chamber to maintain purity. All of the other components exist to facilitate this process. Figure 10 provides a cutaway view of the Houghton College PVD chamber as it has been so far constructed.

With the knowledge of the basic layout of the system, the remainder of this chapter shall be devoted to discussing the components of the PVD system, both current and in development.

### 3.2 Vacuum Technology

In order to maximize the purity of the thin film, the deposition must be executed in a vacuum environment, preferably in the high vacuum pressure range or lower. High vacuum is defined by pressures in the orders ranging from  $10^{-3}$  Torr to  $10^{-9}$  Torr according to the American Vacuum Society [15] and is measured by specialized gauges, the Bayard-Alpert Gauge [16] being employed in this project. While high vacuum is typical for film depositions, it is far more advantageous to attain ultra-high vacuum for even greater purity (defined as pressures lower than approximately  $10^{-9}$  Torr, also by the AVS). To attain such pressures, a series of pumps are necessarily attached to the deposition chamber.

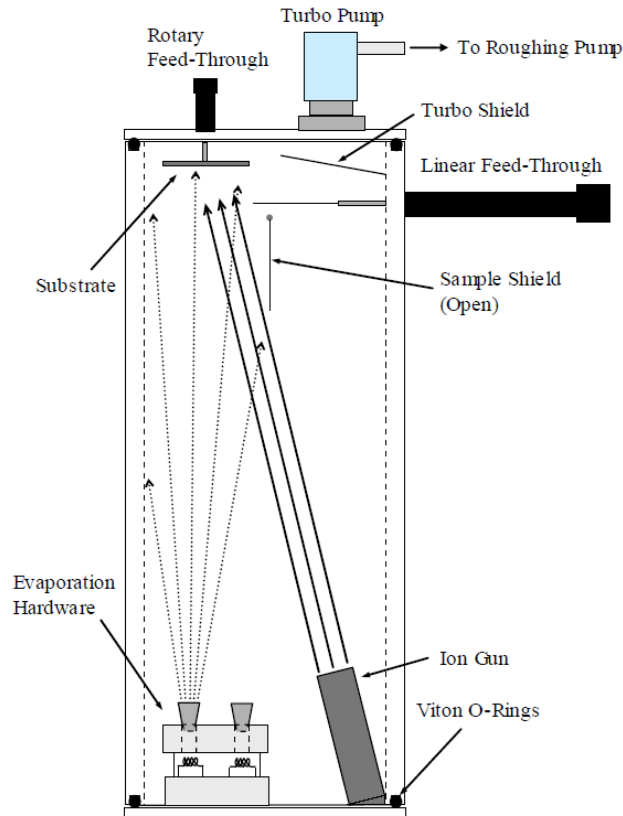


Figure 10: The Houghton College PVD chamber, overviewing the relative locations of the major components. The ERM will be added halfway up the left side of the chamber in this depiction. Figure taken from Ref. [17].

### 3.2.1 Rotary Vane Pump

The first stage of the pumping system at Houghton College is a typical rotary vane pump (RVP), which serves as a roughing pump for the system. The RVP is a mechanical, oil-based pump that hasn't changed much in design since the early twentieth century [18]. Undoubtedly, this pump has the most complex mechanical operation out of the three pumps in the PVD vacuum system and a cross-section can be seen in Figure 11. This pump is responsible for bringing the system to a pressure, approximately  $10^{-3}$  Torr, at which the turbomolecular pump can begin to function, and after which it functions as a backing pump for the same. The RVP is connected to the

turbomolecular pump (and therefore the chamber) through the left input in Figure 11. The gas is taken through the input pipe into the chamber (A) and is pushed through the chamber of the pump (B) in “packets” to (C) where it goes to the output pipe. The ends of the “packet” are sealed by the top of the rotor (3) and the vane (2), which is spring-loaded (4). The output pipe, however, does not go directly to atmosphere. The gas molecules being pumped are released via a one-way valve (5) into an oil reservoir at the top of the pump. Being lighter than the oil, they move to the top of the reservoir and are then able to exit the exhaust valve. This oil reservoir prevents the backflow of atmosphere through the pump and into the system.

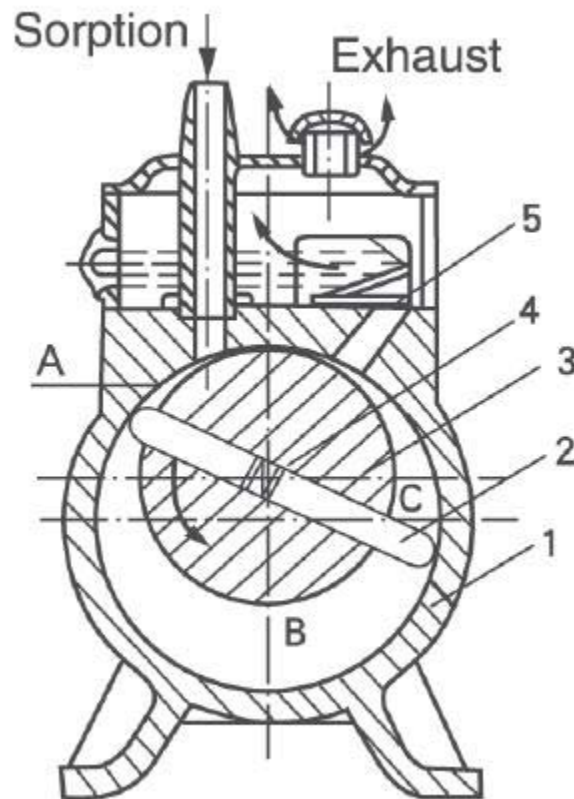


Figure 11: The Rotary Vane Pump. Components are the outer shell (1), the spring loaded vane (2), the inner rotor (3), the spring for the vane (4), and the output valve (5). Figure taken from Ref. [19].

The issue that does arise with the oil reservoir is that the one-way valve does not prevent all oil from escaping back into the main pumping chamber or further into system via the inlet. This is unlikely to cause a problem while the system is held under vacuum, but during venting when the pump is finally shut off, the operator must ensure that the RVP inlet is closed off from the rest of the PVD system so as to not risk oil vapor flowing back into the system.

### 3.2.2 *Turbomolecular Pump*

In order to reach lower pressures than are possible with a typical rough pump such as the rotary vane pump employed in this project, another pump technology is necessary in the system. For the necessity to efficiently reach higher vacuum, the modern turbomolecular pump, or simply the turbo pump, was invented by Becker in 1958 [20].

The basic operating principle of the turbo pump is an evolutionary cousin to the turbojet engine. The operating principle of alternating rotating and stationary blades causes gas molecules to flow at high velocities in one direction. Figure 12 exhibits this blade alteration inside of a turbo pump and Figure 13 displays a cutaway view, showing the blades and motor. The turbo pump is powered from an external supply.

Turbo pumps do not attempt to seal off the line, but instead rely on the backing pressure and the principle of kinetic pumping. Since the quantities of ambient molecules are significantly lower due to the low pressure, it makes less sense to speak of the medium being pumped as a gas or a fluid, but rather as individual non-interacting molecules, similar to a classic ideal gas. As these molecules enter the turbo pump on the chamber side during normal operation, the blades will impact them and redirect them through the pump and towards the external side of the pump. Since the blades are spinning at the high rate of 90,000 rpm, or 1,500Hz, during normal operation [21] there is little chance of molecules travelling the reverse direction through the pump without being imparted with the correct velocity by a rotor blade.

Reaching and maintaining operation at such high rotational speeds while maintaining a vacuum environment requires a unique set of bearings. Since lubricating the chamber-side rotor axle bearing would be detrimental to creating a high-vacuum environment, the designers of the turbo

pump decided to mount this end of the axle without using lubricant. To overcome this problem, the chamber-side axle bearing is an electromagnetic, or “floating,” bearing. Inside this magnetic field, there is still a mechanical bearing, but it is dry and it is only contacted when the rotor is shocked, in order to stabilize it, or out of balance, in which case operation should cease in order to prevent further damage to the pump. In higher-end turbo pumps, the magnet is typically “smart” as well, in a sense that it uses distance sensors and digital signals to make minor corrections and balance the rotor’s motion. [21]

However, the turbo pump cannot operate on its own—it requires another pump to provide an “external,” or backing pressure that is significantly less than that of the atmosphere. Attempting to pump gases at or near atmospheric pressure induces significant stress on the pump components and can lead to irreparable damage to the pump. For this reason, the turbo pump is placed in the system line between the RVP and the chamber. In the event that a significant overpressure does occur, possibly due to a leak in the chamber, inventor William Becker in [21] describes integrated safety features that are built into turbo pumps such as braking by safety bearings. However, it is best practice to construct a system in which these safety measures are rarely, if ever necessary. This is done by ensuring that the turbo pump does not operate in overpressure. In the system described in this project, it is recommended to withhold from starting the turbo pump until the system is at pressures of  $10^{-2}$  Torr or less. Preferably, the operator would wait until the roughing pump has brought the system to pressures in the  $10^{-3}$  Torr range as the lesser the backing pressure, the further the turbo pump will be able to take the system.

The turbo pump in use in the PVD system described here is the Pfeiffer Balzers TPU060. It exhibits the characteristic magnetic bearing on the chamber-side, however it relies on traditional bearings on the backing side. Some higher-end turbo pumps exhibit magnetic bearings on both sides, providing optimal rotational freedom and generate significantly less heat energy. Due to the heat energy generated by the turbo pump in use, water cooling is necessary to maintain operating temperatures that will not harm the pumps.

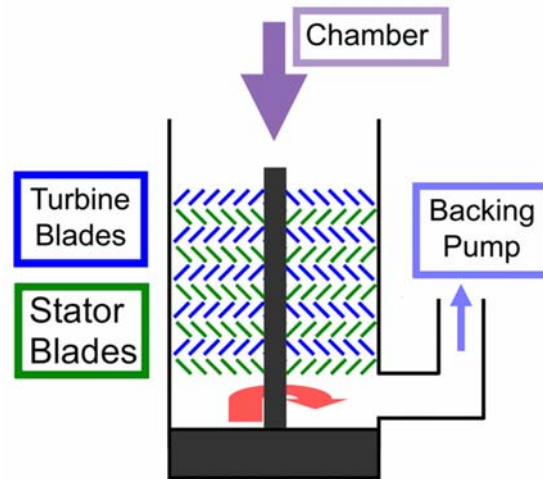


Figure 12: Cross-section diagram of the turbomolecular pump, showing the alternating rotor blades and stationary blades. This enables environments where gas molecules are forced through the pump with little chance of backflow. Figure taken from Ref. [22].



Figure 13: A cutaway of a common turbomolecular pump showing the change in blade size as progressing through the apparatus. Figure taken from Ref. [22].

### 3.2.3 Ion Pump

Future development of the system will include the use of an ion pump to further reduce the pressure in the system beyond that which a turbomolecular pump can achieve. The pump itself has been integrated into the system, but as the focus is currently on the evaporation system, the use of the ion pump has not become part of normal procedure as significant time is necessary to pump down to pressures at which it becomes effective. When it is used, it will allow the production of films with significantly higher purity. The ion pump has no moving parts and operates on the simple principle of applying a high potential difference across ambient molecules. Now ionized, these molecules accelerate towards the wall where they become trapped. The magnetic field induced within the device causes the ions to spiral towards the wall, rather than travelling straight, so that they may ionize other atoms due to collisions in the process of travelling to the chamber wall. The interior concept of the ion pump is shown in Figure 14.

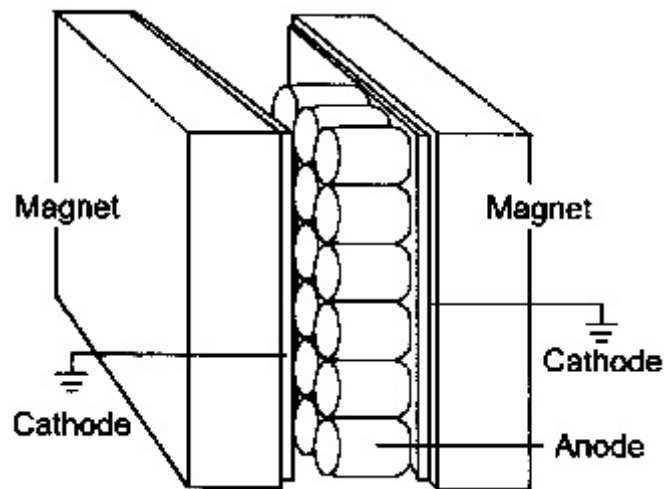


Figure 14: Ion Pump. Molecules enter the apparatus and ionized. The ionized particles are then attracted to the grounded cathode, thereby taking removing them from the chamber's inner atmosphere. Figure taken from Ref. [23].



### 3.2.4 Vacuum Gauges

Necessary to the monitoring of a vacuum system are the gauges in use. The PVD system in development utilizes both a traditional thermocouple gauge for measuring higher pressures as well as a the Bayard-Alpert Ionization Gauge, meant for measuring pressures in the high-vacuum range and lower.

The thermocouple gauge operates on the premise of energy dissipation from a filament due to radiation. Simply, the gauge contains two major components. A heating filament and a thermocouple placed a known distance away calibrated to measure its relative temperature. If the filament voltage is held constant, then the premise is that in constant atmosphere, the thermal radiation from it should be constant. However as the pressure drops and the gas molecules become sparser, the thermal energy radiated by the filament through the gas will decrease causing the temperature measured by the thermocouple to drop. This allows the thermocouple gauge to be accurate down to approximately  $10^{-4}$  Torr, at which a new gauge must be utilized. [18]

At pressures in the high vacuum range, the standard method is to use the Bayard-Alpert Gauge [24] to measure pressure. This gauge functions by the use of an anode and cathode. Residual molecules of gas are ionized in the gauge by the anode and then are electromagnetically accelerated to the cathode. As they collide with the cathode, the current read from the cathode will change. If calibrated correctly, the amount of fluctuation in current will correspond directly to the quantity gas molecules in a given area available to be ionized, thus disclosing to the operator the pressure inside the gauge. Being that the gauge is connected directly to the vacuum chamber, this provides a very accurate reading of the chamber's internal pressure well into the ultra-high vacuum range. The one downside to this gauge is that it is not reliable at pressures in the  $10^{-3}$  Torr range and higher due to an overabundance of molecules being ionized. For this reason, it is best used in a system in tandem with a thermocouple gauge.

### 3.3 Internal Components

In 2007, the Hoffman Research Group began work on components of a PVD system that has at the current stage been assembled and is undergoing tests of the deposition system.

#### 3.3.1 Evaporation Block

Key to any PVD system is a component that can be called the evaporation block. This block is seen in Figure 15 below. Inside this block is a simple system of a filament and crucible, in which the deposition material is placed. The filament has a current through it at a relatively low potential difference and the crucible is grounded. The filament is then floated at a negative potential of several kilovolts, which causes the electrons to travel from the filament to the crucible, a process called thermionic emission. These travelling electrons will transfer their kinetic energy to the crucible when they hit it and it will be converted to thermal energy. This heat is transferred to the deposition material and causes it to heat up. Higher current in the filament causes more electrons to exit the filament and bombard the crucible. The higher in magnitude the floating voltage is, the stronger attraction electrons will have to the crucible. Therefore the electrons will also travel at a greater velocity, thus bombarding the crucible with a higher kinetic energy. This velocity (in meters per second) can be found via a rearrangement of the conservation of energy for the electron's energy:

$$E_e = |q_e|V = \frac{1}{2}m_e v^2 \quad (5)$$

$$v = \sqrt{\frac{2|q_e|V}{m_e}}. \quad (6)$$

In the equation,  $q_e$  is the charge of an electron,  $V$  is the potential difference from the filament to the crucible, and  $m_e$  is the mass of an electron [25]. Therefore the faster heating will occur and the higher temperatures will be able to be reached in the crucible.

Tungsten wire was used to construct the filament due to its extremely high melting point. The decision was also made originally to make the posts out of molybdenum due to its high melting

point and lower cost than tungsten. These were not made out of tungsten because costs would be far too high and due to the thickness of the posts, a weaker material could be used. The two tungsten-molybdenum connections of the filament to the posts posed a great challenge when assembling. Due to the materials' high melting points, spot welding was difficult, but was eventually achieved after using custom fabricated molybdenum leads on the spot welding tool. After the difficulty of the construction of this tungsten-molybdenum filament system, it was decided that the next time the filament was replaced, the filament posts would be replaced with steel for ease of filament repair in the future. Because of the thickness of the posts, steel could be used as heat distribution is greater than in the filament wire itself.

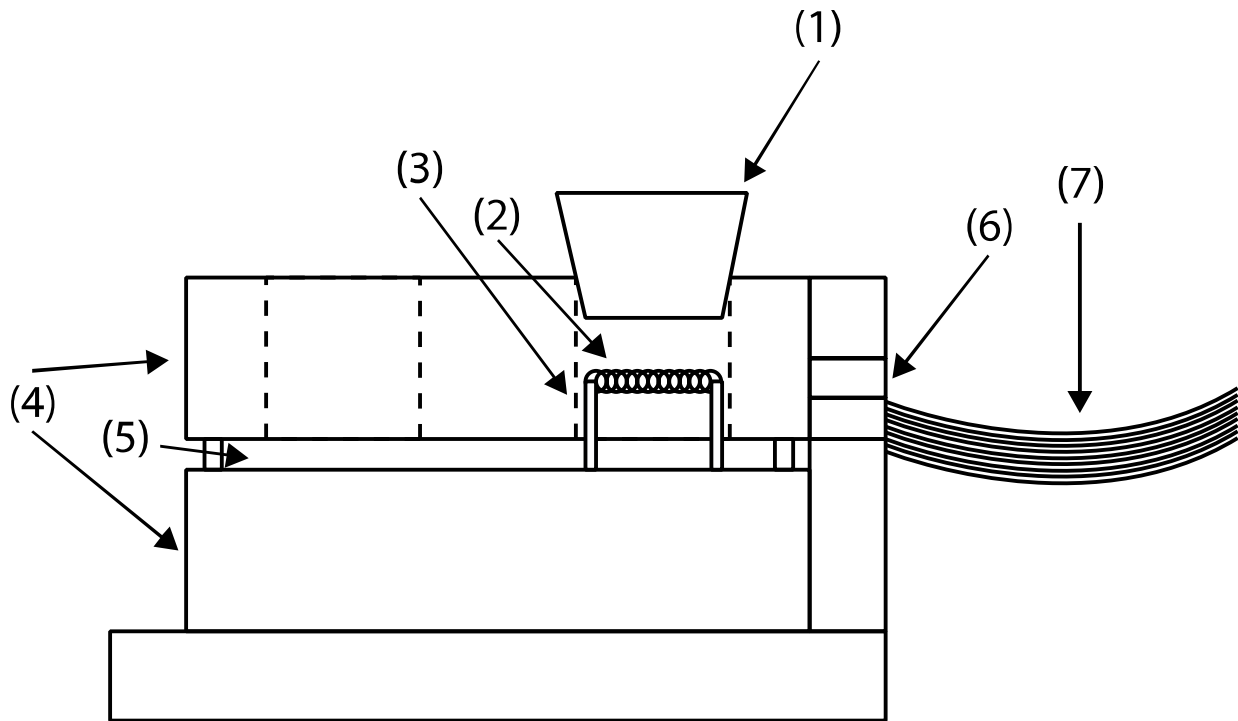


Figure 15: The deposition block system. Main components include the crucible (1), tungsten filament (2), molybdenum filament posts (3), ceramic blocks (4), insulating gap (5), DB-9 electrical connection (6), ribbon cable leading to chamber HV electrical feedthrough.

The block is composed of several different layers of material which should provide for the evaporation of the deposition material in a very efficient manner. As it is preferred to contain the

energy absorbed by the crucible, it was decided to make the structure itself out of ceramic because it is non-conductive and also in order to prevent energy dissipation from the crucible through conduction.

The block (not including the crucible and silver) is constructed to have a detachable section which connects electrically to the base and further to the chamber's high-voltage electrical feedthrough via a DB-9 connection. This connection and base-block system enables the user to remove the ceramic portion of the block to perform maintenance on the filaments or add deposition material without disconnecting all of the hard electrical feedthrough connections. The method in which this removal is done is by detaching the bottom window of the chamber.

As the voltages and currents of filament-crucible heater systems are highly dependent on the construction of the electrical circuit, the actual recommended values must be determined experimentally, which is described in a later chapter.

### *3.3.2 Sample Substrate Heater/Holder*

For the PVD process, it is required for the chamber to contain a mount for the substrate on which the sample will be collected. For the purposes of this project, it was also desired to be able to heat the sample in order to manipulate the structure of the crystal lattice without taking it out of the vacuum in which it was deposited. The design was conceptualized to make the sample heater and the substrate mount one in the same.

Pictured in Figure 18, the sample substrate holder and heater (SSH) apparatus is a fairly complex construction. The main structure is an aluminum plate and this is attached to the exterior of the chamber. All of the components for the SSH system are mounted to this aluminum plate.

The sample (black) is held on notched ceramic posts. These posts are attached to a central ceramic axle. These portions are made of ceramic in order to ensure that the heat conducted away from the sample substrate is minimized. This axle is mounted onto the axle of a rotary feedthrough so that the sample substrate can be rotated from the chamber's exterior while under vacuum.

The heating disc itself is made of ceramic as well because it is a very good electrical and thermal insulator. Wound through this ceramic disc is a long tungsten wire, which acts as a filament for heating. Initially, this filament was configured in a simple threading pattern as outlined in Figure 16, but then was later modified to the style of Figure 17 for ease of filament replacement upon burnout [26].

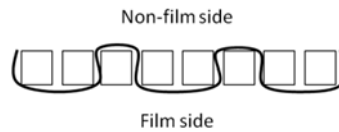


Figure 16: Initial method of filament threading through the sample heater disc. The filament is one continuous wire. The entire disc heats up relatively evenly in this configuration. Figure taken from Ref. [26].

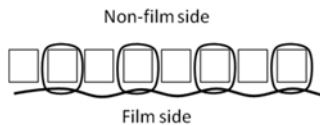


Figure 17: Alternate method of filament threading through the sample heater disc. The filament is made of many wires; each small loop is a single wire and then the main wire on the film side is threaded through those loops in a spiral fashion. Current is only run through the main wire. This configuration favors heat on the film side of the disc. Figure taken from Ref. [26].

This filament is heated and since it is near the sample, the radiant heat causes the sample and substrate to heat up, fairly evenly. This disc does not rotate though; it is fixed by three long ceramic posts to the underside of the aluminum plate that has the rotary feedthrough mounted to it.

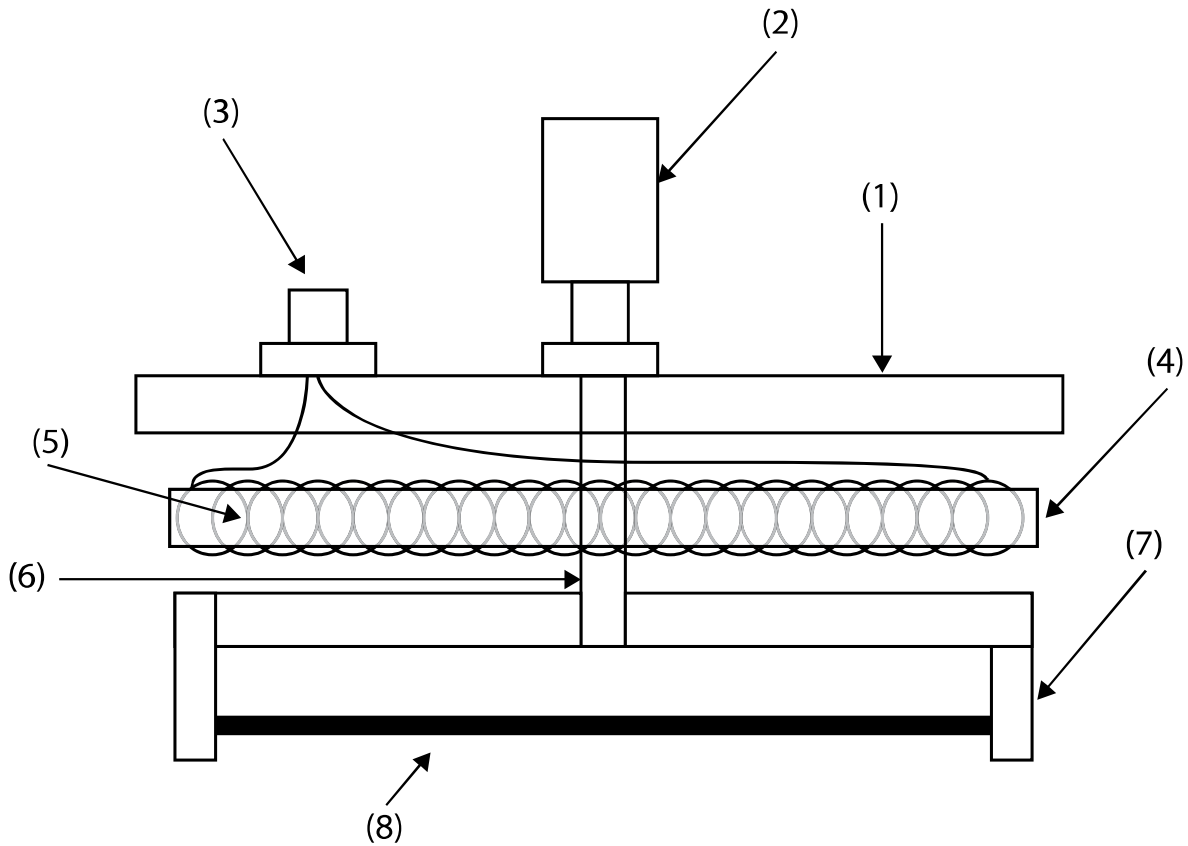


Figure 18: The Sample Substrate Holder/Heater Assembly. Components are the aluminum mounting plate (1), the rotary feedthrough (2), the electrical feedthrough (3), the ceramic heater disc (4), the heater coiling (5), the ceramic axle mount (6), the ceramic wafer-holder arms (7), and the substrate wafer itself (8).

A few components accompany the task performed by the sample heater, namely the heat shield that prevents thermal energy from radiating from the sample heater system down into the rest of the chamber. This infrared filter is mounted on a linear feedthrough so that the sample can be unblocked in the deposition process and is depicted in the full-chamber diagram in Figure 10. It is a unique mirror in that it reflects infrared electromagnetic radiation, but allows the passage of visible light so that the beam from the interferometer can reach the sample and reflect back through uninhibited. Without the concern of allowing the interferometer laser to pass through, the shield above the sample heater and the skirt around it are constructed out of molybdenum plate, as to

prevent heat from dissipating up to the chamber lid and horizontally to the chamber walls. This containment of the heat energy is crucial as the chamber as a whole must be kept at a relatively constant temperature to prevent both further outgassing and distortion of data if the optics were to gain significant thermal energy. Thermal radiation from the heater is enough to affect these optics even though they are mostly outside the chamber; hence the radiation shielding. The other benefit of this shielding is that for the most part it prevents the uneven dissipation of heat, allowing the sample to heat up with relative uniformity.

### 3.3.3 *Evaporation Rate Monitor*

When analyzing thin films, one of the most difficult tasks is to measure how thick the films are. There are several ways this measurement is performed, during or after the film's deposition. A common method of measurement post-deposition is to use a quartz crystal microbalance, also referred to as a crystal rate monitor [27]. The premise of these crystal monitors are two electrodes with a piezo-electric quartz crystal in between. Using an external oscillator, the quartz is made to oscillate at its resonance frequency. As material is deposited on the crystal, it begins to oscillate at a changed frequency due to the same input energy with added mass of deposition material. This change in mass  $\Delta m$  will cause the frequency to change  $\Delta f$  proportionally according to the relationship given in the following equation, where  $f_0$  is the fundamental resonant frequency of the quartz crystal,  $A$  is the active piezo-electric area,  $\rho_q$  is the density of quartz and  $\mu_q$  is the shear modulus of quartz.

$$\Delta f = -\frac{2f_0^2 \Delta m}{A(\rho_q \mu_q)^{1/2}} \quad (7)$$

As mass is deposited on the crystal, over time the problem of too much deposited mass will cause the crystal to fall out of calibration and become unreliable due to the variable extra material not being included in the system calibration. Unfortunately, this is not something that can easily be corrected for because the measurement depends on the crystal's adherence to specific electrical characteristics, with a tolerance. Once this tolerance of variation in electrical properties is breached, the frequency at which the crystal oscillates becomes unstable and therefore unreliable. This

depreciating requires the operator to replace the crystal after several depositions, which makes maintenance of the device costly and frequent.

Another method of rate monitoring used mass spectroscopy [27]. In this method, a mass spectrometer is set up such that all or some of the evaporated deposition material passes through it in order to measure the fraction of the gas that is comprised of the deposition material. This method is considered very intrusive and may not reliably inform the operator of the actual thickness of the film due to its manipulation of the evaporated material.

There are many other methods of monitoring evaporation rate described in [27], but the Hoffman Group has decided to utilize an experimental device, known as an Evaporation Rate Monitor (ERM) described in a paper written by G.R. Giedd and M.H. Perkins, published in 1960 [28]. To the group's knowledge, this is a device that has not been employed as of yet in a PVD chamber. That being said, the use of this device is an experiment in and of itself.

The ERM follows the design given in Figure 19. This device is mounted in such a way that the evaporated material passes into it on a direct vector from the crucible. As the material enters the cylinder that comprises the anode, which is held at a high positive voltage (Giedd and Perkins recommended +155V) and is ionized with a positive charge by the filament (40mA). This is then accelerated towards the collector, which is held at a negative voltage (-20V). These voltages were determined by Giedd and Perkins using the geometry given in Figure 19 using the following two equations and a maximized ionization probability  $P=0.26\%$ :

$$P = 3.95 * 10^{11} J \sigma L \left( \frac{M}{T} \right)^4 \quad (8)$$

$$P = M I_m * \frac{10^{-8}}{N d A p e} \quad (9)$$

where  $J$  is the electron current density,  $\sigma$  is the molecular cross section,  $L$  is the electronic beam length,  $M$  is the molecular mass,  $T$  is the furnace temperature in Kelvins,  $M$  is the molecular weight of the evaporant,  $I_m$  is the ion current of the evaporant,  $N$  is Avogadro's Number,  $A$  is the area of



the collector,  $\rho$  is the density of the metal,  $e$  is the electronic charge, and  $d$  is the evaporation rate. This evaporation rate is the slope of the thickness (and deposited material) versus the time that the evaporation has been running.

As the material bombards the cathode, its charge causes small fluctuations in the current that is read from the collector. This current can be used to determine the rate at which ionized evaporated particles are hitting the collector, which is used to infer the rate at which the particles are hitting the substrate.

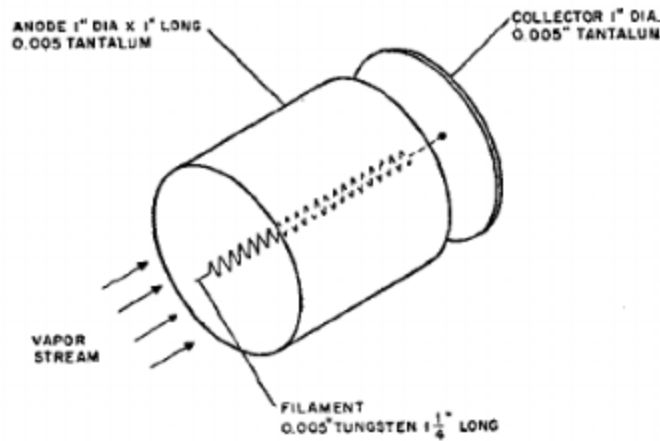


Figure 19: Evaporation Rate Monitor. Major Components include the anode, collector, tungsten filament, and the ceramic base (not shown) Figure taken from Ref. [28].

One potential problem that this system shares with the crystal rate monitor is the buildup of silver on the collector, but this is something that theoretically should not tamper with the accuracy of the device unless the collector begins to contact the anode. Material however would take a significant amount of time to build up given the moderate gap in between the collector and the anode. Given an average film thickness of 1500nm, it would take 2000 depositions to fill a 3mm gap. Certainly, this could not become a problem for many years once depositions become a routine

procedure. The components, as they are foil and wire, are inexpensive to replace when it becomes necessary.

The larger issue that comes up with using the monitor is based on the atmosphere within the PVD chamber. According to the authors proposing the Evaporation Rate Monitor 28, for chamber pressures greater than  $10^{-5}$  Torr, a correction must be accounted for when determining the ion current caused by the metal vapor  $I_m$ :

$$I_m = I_r - I_g, \quad (10)$$

where  $I_r$  is the measured ion current from the rate monitor and  $I_g$  is the ion current caused by the non-evaporant residual atmosphere inside the chamber. However, for pressures smaller than this, the authors note that this correction may be considered negligible.

At the time of this writing, the circuitry designed by Giedd and Perkins has not been constructed, so the device is not yet ready for testing. With all of the factors taken into account, the Hoffman group will test the evaporation rate monitor against thickness measurements from another device, such as an atomic force microscope or a film thickness profilometer to determine if it is a viable method of measuring deposition rate and implied film thicknesses.

#### 3.3.4 *Ion Mill*

The system also includes an “ion gun” cleaning device, but it is not yet in use. The model is a Commonwealth Scientific Company Mark I ion mill, shown in the base of Figure 10. This works by the simple concept of forcing a controlled leak of nitrogen or argon gas into the chamber towards the substrate at a high velocity, using an effect similar to that of a sand blaster, with a key difference. To use the ion mill, the chamber is filled to rough vacuum with an inert gas such as argon. As the gas molecules behave close to that of an ideal gas in this low-pressure environment, there is no bias as to their direction of travel. The gun generates an electric field in a tight vector and causes the gas to ionize and accelerate towards and bombard the substrate. These ions will be abrasive to the substrate surface, causing excess contaminant, corrosion, and other impurities to be kinetically removed. The residual gas is then pumped out of the chamber to complete the cleaning process. [29]

### *3.3.5 Rotary and Linear Shutters*

Two key shutters are present within the chamber. Seen in Figure 10, these are the rotary and linear shutters. The rotary shutter allows the operator to quickly (manually) shield and unshield the substrate from the evaporant in the chamber. This is important as the intended evaporant takes time to reach the desired rate as well as one of the first components to evaporate is the oxidation layer on the deposition material. It is desired to avoid this contaminant's presence in the sample film in any quantity, thus the importance of being able to block the substrate. This shield also allows the user to "cut off" the deposition at the desired thickness rather than having to account for material evaporated and deposited during the cooling stage of the evaporator after it has been turned off. The second shutter is a linear shutter which allows the operator to deposit a gradient film. As deposition is occurring, the shutter slowly covers the sample, allowing several thicknesses of film to be deposited on the same substrate in the same run.

## **3.4 Suspension of System**

One of the ultimate goals is to be able to perform in-situ observations of films during both growth and annealing phases via a mounted laser interferometer. This is a very precise measurement system and requires the utmost consideration of the effects of the surrounding environment, particularly vibrations that are inherent of the building that contains the system. Because of this, the entire vacuum chamber and interferometer will be suspended on a spring-frame system as to limit vibrational and resonance effects from the environment that the instrument is in, as depicted in Figure 21. This increases the overall size of the system drastically as the outer frame measures three feet square by seven feet tall.

## **3.5 The Interferometer**

As the Twyman-Green Laser Interferometer is a driving factor of the construction of the frame system as well as the primary measurement instrument for the films while under vacuum, it is necessary to give a brief overview of it.

The optics apparatus used employs the characteristics of lensing to build an advanced interferometer that can study a portion of a surface three inches in diameter. This interferometer was built on an optics table, or a steel table with a grid of threaded holes. An optics table is used because of its versatility, mainly the user's ability to add, move, or remove items from it by simply using a screwdriver. The basic optics setup of the interferometer is given in Figure 20.

This assembly works using the emission of a uniform light beam from a 25mW class IIIb laser. The beam passes through two concave diverging lenses to spread the beam out and then through the beam splitter to cause half of the beam to travel towards the reference mirror (the lower mirror in Figure 20) and half through a window into the chamber (shown here with a mirror—used for testing purposes). Before the spreading beam reaches either location, it passes through a collimating lens. These convex lenses collimate the beam into one cylindrical beam with an approximate three inch diameter. One beam then reflects back off the permanent mirror, is converged by its respective collimating lens and reaches the beam splitter. The beam passes through the window at the bottom of the chamber, reflects off the sample, passes through its respective collimating lens again, and then returns to the beam splitter as a converging beam. Both the beams meet up in the beam splitter and they interfere with each other. The beam splitter will direct these beams both towards the laser and also towards whatever surface or device the operator is using to observe the results. A mirror directs the beam to a screen and in the camera-captured image, the operator is able to see lines of interference that represent the topography of the sample inside the chamber.

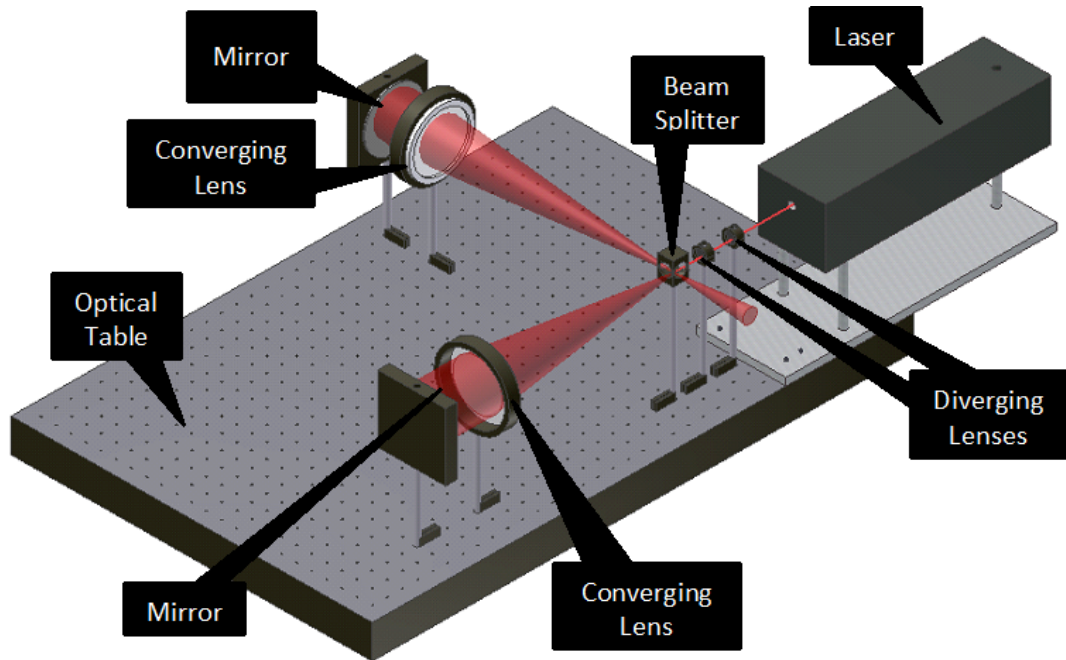


Figure 20: The Twyman-Green interferometer basic optics setup. A camera will be added in future development in order to digitally and actively record interference patterns.

The optics assembly will sit underneath the chamber, tilted vertically so that collimating lens 4a in Figure 4 will be in line with the window in the bottom of the chamber. This will allow the three inch diameter beam of the interferometer to “view” the sample through the deposition chamber. A three-dimensional model of the entire system can be seen in Figure 21. This image shows an open interferometer. In reality, the interferometer was enclosed in a wooden box, with a hole cut in it for the beam. This was done to minimize the effect of air currents and ambient light.

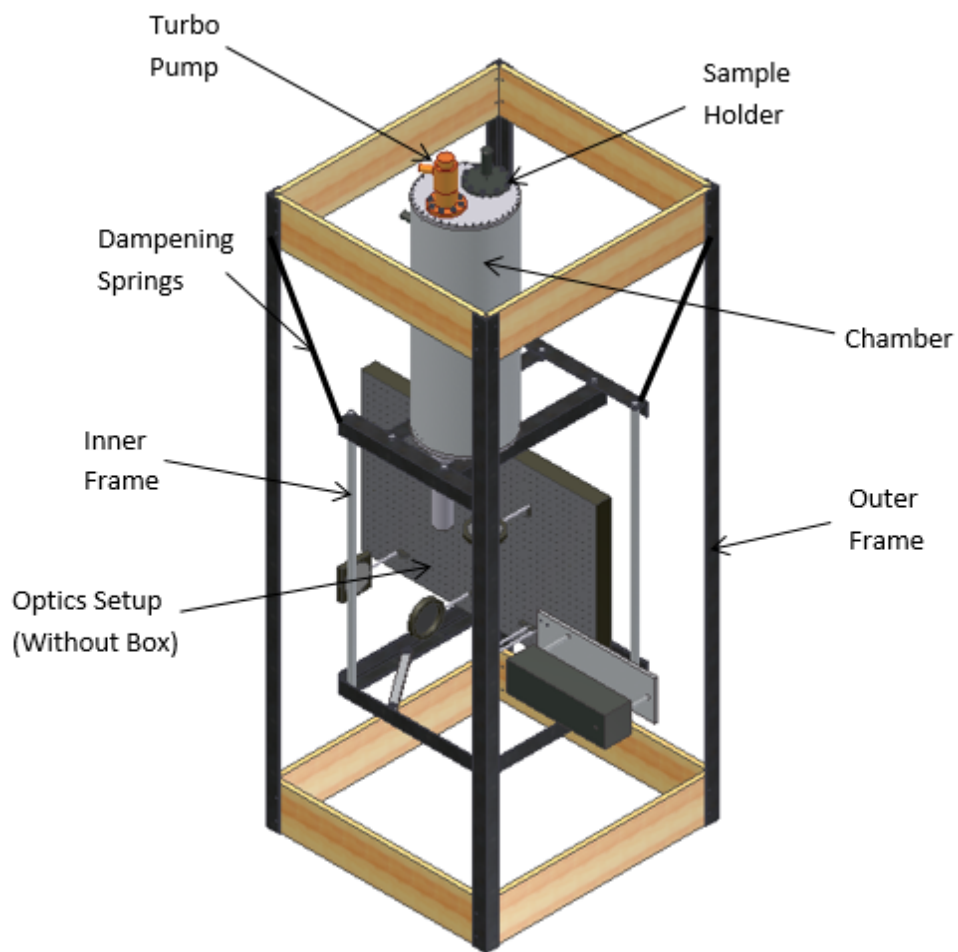


Figure 21: The mounted chamber and interferometer. The instrumentation is mounted on an inner frame, which is hung on heavy springs from an outer frame. Note that the original outer frame (depicted here) has wooden horizontal members; these have been since reconstructed out of aluminum. All other members of the frames are made of 1/4" thick angle steel. The entire outer frame measures approximately seven feet tall.

## *Chapter 4.*

### CURRENT STATUS OF THE PROJECT

#### **4.1 Overview**

Two primary tests were conducted during this phase of the project. The first of which was to ensure that the PVD chamber could maintain high vacuum with all of the instruments and feedthroughs that were added to the bare chamber. Repeated each time the configuration of the chamber was changed, these tests were largely qualitative but success was determined if the chamber could reach pressures in the  $10^{-6}$  Torr range using the roughing pump and the turbo pump. Each time, a specific procedure was followed, given in Appendix A. The second test, that at the time of this writing has not been completed is to determine the proper floating voltage and current for the filament which is used to vaporize the deposition material via the process of thermionic emission.

#### **4.2 Components Remaining to be Completed**

The components with physical construction remaining to be completed in the construction of the PVD system include the circuitry for the rate monitor, the final design of the exterior deposition filament control circuitry, and the various shields and shutters inside the chamber.

The rate monitor circuitry is exemplified in theory by Geidd and Perkins 28, so the remaining design work necessary is to develop a plan for its physical construction and subsequently build and calibrate it. Calibration of this system will require the ability to deposit films as results from the rate monitor must be calibrated to measurements taken on another pre-calibrated device, such as a profilometer or atomic force microscope.

Temporary circuitry has been constructed for the deposition filament controller, but for long term use of the system, a more compact and purposeful circuit must be constructed or purchased that is both safe and reliable. Safety must be taken into the account when designing this controller as the voltage of the thermionic emission filament is necessarily floated over a thousand volts.

## *Chapter 5.*

### CONCLUSIONS

Throughout this project much rework has been necessary as problems arose. Often, time would be required to determine sources of vacuum leaks and repairing the system as necessary. The major setback in this project was that the entire system had to be moved twice to accommodate construction in the building which houses it. When working with components that require high precision, the total disassembly/reassembly process causes significant wear on them.

However, the priority moving forward will be the calibration of the deposition system itself. The proper voltages for the thermionic emission system will allow the operators to efficiently and quickly vaporize all varieties of deposition material with a localized heating application. Also a part of this system, the evaporation rate monitor circuitry will need to be constructed, which could be an entire project by itself due to its intricacy. Proof of the viability of this method for determining film growth rate will be a significant development in the scientific field of vacuum deposition.

After several years of development, the PVD system at Houghton College is nearing the point at which it will be operational for use in producing films for study using both the onboard interferometer as well as external instrumentation such as an x-ray diffractometer and an atomic force microscope.



APPENDIX I  
PROCEDURE FOR USE OF VACUUM CHAMBER

**AI. 1 Pump-Down Procedure**

Pumping down the chamber is a process of several steps. In list form, the steps are:

1. Ensure that all exterior valves and vents are closed and that all components are securely and properly attached. No hole in the chamber should be left uncovered. The butterfly valve between the turbo pump and the chamber should remain open.
2. Turn on the roughing pump. Wait a few moments and then open the roughing pump valve located between roughing pump and the turbo pump. This waiting period is crucial to ensure that there will not be backpressure into the chamber, potentially causing oil vapor to enter the turbo pump or the chamber.
3. Wait approximately ten minutes or longer for the whole system to pump down to  $10^{-2}$  Torr or lower. The lower, this initial pumping goes, the better results the operator will have in the next phase.
4. Ensure that the coolant travelling through the turbo pump housing is flowing. It may be going very slowly to conserve coolant and pumping energy, but it is critical to be kept flowing to prevent the turbo pump from overheating. Turn on the turbo pump. It should take approximately five to ten minutes to spin up to its operating speed of ninety thousand RPM.
5. Wait until the desired pressure is reached. If necessary, heat the chamber to bake off inner atmospheric residue using heater tape (remember the coolant must be flowing through the turbo pump). Note that the best performance seen with the system in the spring of 2013 was  $10^{-7}$  Torr after a two day pumping that included sixteen hours of baking.
6. Once the desired pressure is reached, film evaporation may begin.

## **AI.2 Venting Procedure**

A strict procedure must also be followed during venting to ensure the proper maintenance of the system. The procedure is as follows:

1. Turn off the turbo pump and let it begin to spin down. As the pump is spinning down, open the turbo vent as it goes through resonance frequencies to pass through these frequencies faster and cause less wear on the rotor and bearings.
2. Close the valve between the roughing pump and the turbo pump. This is to ensure that oil vapor from the roughing pump does not enter the rest of the system. At this point, the roughing pump may be turned off.
3. This step is optional, but recommended. As the turbo pump spins through its resonance frequencies (this is known because it becomes very loud), open its relief valve and then close it once it's through its resonance frequency. This is to limit the vibration that the blades are subjected to.
4. Once the turbo pump is nearly spun down (almost quiet) open the turbo pump's relief valve and this will allow the chamber to vent, except the hose between the roughing pump and its valve (this is normal to leave partially under vacuum).
5. Once fully vented, the chamber may be opened.

## References

---

- [1] Milton Ohring, *Materials Science of Thin Films* (Academic Press, San Diego, 2002).
- [2] Vikas Patil, *Journal of Surface Engineered Materials and Advanced Technology*, **2011 (1)**, 37 (2011).
- [3] Katherine Bourzac, MIT Technology Review Online (2010).
- [4] L.B. Freund and S. Suresh, *Thin Film Materials Stress, Defect Formation, and Surface Evolution*. (University Press, Cambridge, 2009).
- [5] W.R. Grove, *Philosophical Transactions of the Royal Society*, **142**, 87 (1852).
- [6] M. Faraday, *Phil. Trans.*, **147**, 145 (1857).
- [7] M. Plücker, *The London, Edinburgh, and Dublin Philosophical Magazine*, **16**, 409 (1858).
- [8] T.A. Edison, *Apparatus for Vacuously Depositing Metals*, US Patent 767,216 (1904).
- [9] D.M. Mattox, *The Foundations of Vacuum Coating Tech.* (Noyes/William Andrew, Norwich, 2003).
- [10] Intel, Ivy Bridge Platform Brief, (2013).
- [11] Micah Baker and Hobble Cohen, Report for the University of Maryland, 2004.
- [12] C.V. Thompson, *Materials Science & Engineering*, **B32**, 211 (1995).
- [13] Aaron Vodnick, *Acta Materiala*, **58**, 2452 (2010).
- [14] R. Carel, *Acta Materiala*, **44**, 2479 (1996).
- [15] <http://www.aip.org/avsguide/refguide/glossary.html>.
- [16] K. Jousten, CERN, (2007).
- [17] K. Aikens, Undergraduate Thesis (Houghton College, New York, 2009, unpublished).
- [18] Saul Dushman, *Production and Meas. of High Vac.* (General Electric Review, Schenectady, 1922).
- [19] [http://www.sfpumps.com.cn/en\\_ProductShow.asp?ProductID=43](http://www.sfpumps.com.cn/en_ProductShow.asp?ProductID=43).
- [20] Robert M. Besancon, *The Encyc. of Physics, 3rd Ed.* (Van Nostrand Reinhold, New York, 1990).
- [21] W. Becker, *Turbo-Molecular Pump*, US Patent 3,477,381 (1969).
- [22] [http://en.wikipedia.org/wiki/Turbomolecular\\_pump](http://en.wikipedia.org/wiki/Turbomolecular_pump).
- [23] <http://www.cae2k.com/howto.html>.
- [24] K. Jousten, CERN, (2007).
- [25] Donald L. Smith, *Thin-Film Deposition: Pri. and Prac.* (McGraw-Hill, New York, 1995), p. 376-377.
- [26] A Silvernail, Undergraduate Thesis (Houghton College, New York, 2011, unpublished).
- [27] Christiana Buzea, *Reports on Progress in Physics*, **68**, 385 (2005).
- [28] G.R. Geidd and M.H. Perkins, *The Review of Scientific Instruments*, **31 (7)**, 773 (1960).
- [29] Steve I. Petvai, *Method for cleaning surfaces by ion milling*, US Patent 4,278,493 (1981).